

# Sterile neutrino dark matter via coinciding resonances

J. Ghiglieri<sup>a</sup> and M. Laine<sup>b</sup>

<sup>a</sup>*SUBATECH, Université de Nantes, IMT Atlantique, IN2P3/CNRS,  
4 rue Alfred Kastler, La Chantrerie BP 20722, 44307 Nantes, France*

<sup>b</sup>*AEC, Institute for Theoretical Physics, University of Bern,  
Sidlerstrasse 5, CH-3012 Bern, Switzerland*

## Abstract

It has been proposed that two resonances could coincide in the early universe at temperatures  $T \sim 0.2 \dots 0.5$  GeV: one between two nearly degenerate GeV-scale sterile neutrinos, producing a large lepton asymmetry through freeze-out and decays; another between medium-modified active neutrinos and keV-scale sterile neutrinos, converting the lepton asymmetry into dark matter. Making use of a framework which tracks three sterile neutrinos of both helicities as well as three separate lepton asymmetries, and scanning the parameter space of the GeV-scale species, we establish the degree of fine-tuning that is needed for realizing this scenario.

## Contents

<b>1</b>	<b>Introduction</b>	<b>1</b>
<b>2</b>	<b>Review of framework</b>	<b>2</b>
<b>3</b>	<b>Low-energy constants</b>	<b>3</b>
<b>4</b>	<b>Parameter scans</b>	<b>5</b>
4.1	Numerical results . . . . .	5
4.2	Analytic estimates . . . . .	7
<b>5</b>	<b>Example of a successful solution</b>	<b>10</b>
<b>6</b>	<b>Conclusions</b>	<b>11</b>

## 1. Introduction

It has been a long-standing dream that a theoretical and experimental understanding of the mechanism of neutrino mass generation could also help to solve outstanding cosmological mysteries, such as the existence of baryon asymmetry and of dark matter abundance.

In the present paper we approach this dream from a minimalistic and phenomenologically oriented perspective. The existence of non-vanishing neutrino masses can be accounted for by incorporating right-handed neutrino fields in the Standard Model Lagrangian,

$$\mathcal{L}_{\text{new-SM}} \equiv \mathcal{L}_{\text{old-SM}} + \bar{\nu}_R i \not{\partial} \nu_R - (\bar{\nu}_R \tilde{\phi}^\dagger h \ell_L + \bar{\ell}_L h^\dagger \tilde{\phi} \nu_R) - \frac{1}{2}(\bar{\nu}_R^c M \nu_R + \bar{\nu}_R M^\dagger \nu_R^c). \quad (1.1)$$

Here  $\tilde{\phi} \equiv i\sigma_2 \phi^*$  is a conjugated Higgs doublet,  $\nu_R^c$  is a charge-conjugated right-handed neutrino field with three generation indices,  $\ell_L$  are the Standard Model lepton doublets, and  $h$  is a  $3 \times 3$  matrix of neutrino Yukawa couplings.

A singular value decomposition permits to write the Majorana mass matrix  $M$  in eq. (1.1) as  $M = O \text{diag}(M_1, M_2, M_3) O^T$ , where  $M_I \geq 0$  can be set in increasing order. In the seesaw regime [1–3], the  $M_I$  are close to the physical masses of sterile neutrino mass eigenstates. In this paper we work under the (unconfirmed) assumption that  $M_1 \approx 7$  keV is the mass of a long-lived dark matter candidate [4,5], whereas  $M_{2,3} \sim$  a few GeV represent short-lived states that decay before primordial nucleosynthesis (cf., e.g., refs. [6,7] and references therein).

The GeV-scale mass range for  $M_{2,3}$  is motivated by many reasons. First of all, it leads to a leptogenesis scenario [8,9] which could be testable through experiments at the intensity frontier, such as SHiP [10]. Second, it leads to an interesting dark matter scenario [11,12], in which the freeze-out and decays of the GeV-scale states play a key role.

More precisely, it is known that if this model is used for baryogenesis, then lepton asymmetry production can continue after sphaleron freeze-out [11, 13], and the final lepton asymmetries can be up to  $\sim 10^3$  larger than the baryon asymmetry [14]. However, as suggested by previous studies [15–17] and confirmed by a precise investigation [18], such asymmetries are still  $\sim 10^2$  too small to produce the correct dark matter abundance through the Shi-Fuller mechanism [19]. The suggestion of refs. [11, 12] is that the missing orders of magnitude could originate from the low-temperature freeze-out and decays of the GeV-scale sterile states.

The purpose of the current paper is, on one hand, to verify that the scenario laid out in ref. [12] can be realized and, on the other, to quantify the degree of fine-tuning that it depends on. To this end, after reviewing the general framework (cf. sec. 2), we define a set of “low-energy constants” (cf. sec. 3) which capture the essential aspects of the low-temperature solution. We then scan the parameter space, establishing the part in which the low-energy constants obtain their desired values (cf. sec. 4). Finally, picking a point from the allowed domain, we show a successful scenario which yields (even a bit more than) the correct baryon asymmetry and dark matter abundance (cf. sec. 5).

## 2. Review of framework

Our study is based on a set of evolution equations for “slow variables” that was established in ref. [18] and confirmed through a rigorous derivation in ref. [20]. In order to permit for computationally expensive numerical scans, we simplify here the equations by momentum averaging the density matrices of the GeV-scale sterile species. This implies that their momentum dependence is assumed to take the form

$$\rho_H^\pm(\mathbf{k}) \simeq n_F(\omega_H) \frac{Y_H^\pm}{Y_{\text{eq}}^+}, \quad Y_{\text{eq}}^+ \equiv \frac{\int_{\mathbf{k}} n_F(\omega_H)}{s_T}, \quad (2.1)$$

where  $\pm$  stands for helicity symmetry/antisymmetry; the subscript  $H$  refers to the “heavy” sterile species;  $n_F$  is the Fermi distribution;  $\omega_H \equiv \sqrt{k^2 + M_H^2}$  with  $k \equiv |\mathbf{k}|$  and  $M_H \equiv (M_2 + M_3)/2$ ; and  $s_T$  denotes the thermal entropy density of the Standard Model degrees of freedom. Inserting eq. (2.1) into the evolution equations, the coefficients appearing in them get averaged in one of two possible ways,

$$\langle \dots \rangle_1 \equiv \frac{\int_{\mathbf{k}} (\dots) n_F(\omega_H)}{\int_{\mathbf{k}} n_F(\omega_H)}, \quad \langle \dots \rangle_2 \equiv \frac{\int_{\mathbf{k}} (\dots) n_F(\omega_H) [1 - n_F(\omega_H)]}{s_T}. \quad (2.2)$$

Averages of the second type, originating in connection with certain terms proportional to lepton chemical potentials, become Boltzmann-suppressed when  $T \ll M_H$ .

An essential aspect of the dynamics is that the GeV-scale species fall out of equilibrium,

i.e.  $Y_H^+ \neq \mathbb{1} Y_{\text{eq}}^+$  and  $Y_H^- \neq 0$ . This also affects the expansion of the universe. Denoting

$$x \equiv \ln\left(\frac{T_{\text{max}}}{T}\right), \quad \mathcal{J} \equiv \frac{dx}{dt}, \quad (2.3)$$

and referring for details to sec. 3 of ref. [18], the upshot is that rate coefficients get normalized through the Jacobian  $\mathcal{J}$ , and the evolution is affected by entropy increase, *viz.*

$$\widehat{C} \equiv \frac{C}{\mathcal{J}}, \quad Y'(x) \equiv [\partial_x + \partial_x \ln(s_T a^3)] Y(x), \quad f'(x, k) \equiv \frac{df(x, k(x))}{dx}, \quad (2.4)$$

where  $a$  is the scale factor and  $\partial_x \ln(s_T a^3) = 3\widehat{H} - 1/c_s^2$ , where  $H$  is the Hubble rate and  $c_s^2$  is the speed of sound squared. Furthermore  $k(x) = k(x_0)a(x_0)/a(x)$  denotes a co-moving momentum. In thermal equilibrium,  $\mathcal{J} = 3c_s^2 H$  and  $\partial_x \ln(s_T a^3) = 0$ .

With this notation, the yield parameters for lepton minus baryon asymmetries evolve as

$$Y'_a - \frac{Y'_B}{3} = \frac{4}{s_T} \int_{\mathbf{k}} \left\{ [f^+ - n_{\text{F}}(\omega_1)] \widehat{B}_{(a)11}^+ + f^- \widehat{B}_{(a)11}^- - n_{\text{F}}(\omega_1) [1 - n_{\text{F}}(\omega_1)] \widehat{A}_{(a)11}^+ \right\} \\ + 4 \text{Tr} \left\{ (Y_H^+ - Y_{\text{eq}}^+) \langle \widehat{B}_{(a)H}^+ \rangle_1 + Y_H^- \langle \widehat{B}_{(a)H}^- \rangle_1 - \langle \widehat{A}_{(a)H}^+ \rangle_2 \right\}, \quad (2.5)$$

where  $a \in \{e, \mu, \tau\}$  and  $f^\pm$  are the distribution functions of the keV-scale sterile neutrinos, for which no momentum averaging is carried out, as their resonant production proceeds one momentum mode at a time. The heavy components of the density matrix evolve as

$$(Y_H^\pm)' = i[\langle \text{diag}(\widehat{\omega}_2, \widehat{\omega}_3) - \widehat{H}_H^+ \rangle_1, Y_H^\pm] - i[\langle \widehat{H}_H^- \rangle_1, Y_H^\mp] \\ + \{ \langle \widehat{D}_H^\pm \rangle_1, Y_{\text{eq}}^+ - Y_H^+ \} - \{ \langle \widehat{D}_H^\mp \rangle_1, Y_H^- \} + 2 \langle \widehat{C}_H^\pm \rangle_2, \quad (2.6)$$

whereas light components satisfy

$$(f^\pm)' = 2D_{11}^\pm [n_{\text{F}}(\omega_1) - f^+] - 2D_{11}^\mp f^- + 2C_{11}^\pm n_{\text{F}}(\omega_1) [1 - n_{\text{F}}(\omega_1)]. \quad (2.7)$$

In eq. (2.7),  $\omega_1 \equiv \sqrt{k^2(x) + M_1^2}$ , and  $k(x)$  also appears in the coefficient functions.

Eqs. (2.5)–(2.7) are parametrized by the rate coefficients  $\widehat{A}_{IJ}^+, \dots, \widehat{D}_{IJ}^\pm$  and the effective Hamiltonians  $\widehat{H}_H^\pm$ . These are proportional to the second power of neutrino Yukawa couplings, and in some cases to chemical potentials (e.g.  $\widehat{A}_{IJ}^+, \widehat{C}_{IJ}^\pm$ ). Some important coefficients are elaborated upon in sec. 3, and all definitions and evaluations are explained in ref. [18].

### 3. Low-energy constants

The slow evolution equations in eqs. (2.5)–(2.7) contain a large number of coefficients that capture the effects of the fast Standard Model degrees of freedom. The physical values of the coefficients are correlated, as all of them originate from a certain retarded correlator of

Standard Model operators [18, 20]. Therefore the qualitative features of the solution only depend on the values of a few coefficients. Motivated by the analogy with effective field theories, we call these coefficients “low-energy constants”.

For lepton chemical potentials large enough that all of dark matter gets produced, dark matter production peaks at  $T \sim 0.2$  GeV if  $M_1 \sim 7$  keV [16]. As most of the lepton asymmetries that were produced at higher temperatures get diluted away [18], their production should take place close to this temperature range [12]. Based on numerical integrations such as that described in sec. 5, we find that it is practical to fix  $T = 0.5$  GeV for considering the values of the low-energy constants.

For producing large lepton asymmetries, CP-violation needs to be resonantly enhanced. This means that the oscillations between the GeV-scale species need to be slow, i.e. with a frequency similar to the Hubble rate. The oscillation frequency is determined by three types of mass-squared differences: (i) Lagrangian parameters,  $M_3^2 - M_2^2$ ; (ii) Higgs vev corrections  $\sim \Delta h^2 v^2$ ; (iii) thermal corrections, which at low temperatures are  $\propto G_F^2 T^4$ , where  $G_F$  is the Fermi constant. At  $T = 0.5$  GeV, corrections of types (i) and (ii) are the most important ones in absolute magnitude, however as it turns out that an exquisite cancellation is required between the different types of corrections, the class (iii) also plays a role (cf. sec. 4.2).

Technically, slow oscillations require that, after subtracting the trace part which has no effect, the Hamiltonian in the first commutator of eq. (2.6) should have a near-zero eigenvalue [12]. This gives us the first low-energy constant, which we define in the limit of thermal equilibrium and vanishing chemical potentials:

$$\begin{aligned} \langle \widehat{H}_\lambda \rangle_1 &\equiv \lim_{\mu_i \rightarrow 0} \left| \text{eigenvalue} \left( \langle \text{diag}(\widehat{\omega}_2, \widehat{\omega}_3) - \widehat{H}_H^+ \rangle_1 - \frac{1}{2} (\text{trace}) \right) \right|_{\mathcal{J} \rightarrow 3c_s^2 H_T} \quad (3.1) \\ &= \sqrt{\left[ \frac{\langle \omega_2 - \omega_3 \rangle_1 - \sum_a (|h_{2a}|^2 - |h_{3a}|^2) \langle U_{(a)H}^+ \rangle_1}{6c_s^2 H_T} \right]^2 + \left[ \frac{\sum_a \text{Re}(h_{2a} h_{3a}^*) \langle U_{(a)H}^+ \rangle_1}{3c_s^2 H_T} \right]^2}, \end{aligned}$$

where  $H_T$  is the contribution to the Hubble rate from (thermal) Standard Model degrees of freedom. The coefficient  $U_{(a)H}^+$  captures the “dispersive” corrections of types (ii) and (iii), and originates from the real part of a matrix element of a retarded correlator [18].

It is not sufficient to have slow oscillations between the GeV-scale sterile species, but suitable interaction rates need also to be present. Interaction rates should not be too large, otherwise the sterile neutrinos stay close to equilibrium and furthermore an efficient washout of any lepton asymmetries takes place. But they should not be too small either, otherwise no interesting dynamics takes place. In short, interaction rates should be of the order of the Hubble rate. As a representative for a CP-even rate coefficient, we define

$$\langle \widehat{\Gamma}_H \rangle_1 \equiv \text{Tr} \langle \widehat{D}_H^+ \rangle_1 \Big|_{\mathcal{J} \rightarrow 3c_s^2 H_T} = \frac{\sum_a \sum_{I=2,3} |h_{Ia}|^2 \langle Q_{(a)H}^+ \rangle_1}{3c_s^2 H_T}. \quad (3.2)$$

The coefficient  $Q_{(a)H}^+$  describes “absorptive” corrections, and originates from the imaginary part of a matrix element of a retarded correlator [18].

Finally, the generation of lepton asymmetries necessitates the presence of CP-violating interaction rates. By inspecting solutions such as that described in sec. 5, we have found that a good representative for them is given by

$$\langle \widehat{\Gamma}_{\text{osc}} \rangle_1 \equiv \lim_{\mu_i \rightarrow 0} \langle i \widehat{D}_{23}^+ \rangle_1 \Big|_{\mathcal{J} \rightarrow 3c_s^2 H_T} = \frac{\sum_a \text{Im}(h_{2a} h_{3a}^*) \langle Q_{(a)H}^- \rangle_1}{3c_s^2 H_T}. \quad (3.3)$$

Here  $Q_{(a)H}^-$  describes a helicity-antisymmetrized absorptive correction. Again, eq. (3.3) should be of order unity for an efficient production of lepton asymmetries.

## 4. Parameter scans

The purpose of this section is to determine the possible values of the low-energy constants in eqs. (3.1)–(3.3). We start with a numerical scan in sec. 4.1, and subsequently explain the results through analytic estimates in sec. 4.2.

### 4.1. Numerical results

In the following we employ the Casas-Ibarra parametrization [21], which ensures that active neutrino mass differences and mixing angles take their observed values. As only two mass differences are known, we can account for the observed values through the two GeV-scale sterile neutrinos. With

$$M_M \equiv \begin{pmatrix} M_2 & 0 \\ 0 & M_3 \end{pmatrix}, \quad R \equiv \begin{pmatrix} \cos z & \sin z \\ -\sin z & \cos z \end{pmatrix}, \quad z \in \mathbb{C}, \quad (4.1)$$

this is obtained through the relation

$$h = -i \sqrt{M_M} R P \underbrace{\sqrt{m_\nu} V_{\text{PMNS}}^\dagger}_{\text{data}} \frac{\sqrt{2}}{v}, \quad (4.2)$$

where  $m_\nu$  is a diagonal matrix containing the active neutrino masses,  $V_{\text{PMNS}}$  is the Dirac-like mixing matrix (which contains the complex phase  $\delta$ ),  $v \simeq 246$  GeV is the Higgs vev, and

$$P_{\text{NH}} \equiv \begin{pmatrix} 0 & e^{-i\phi_1} & 0 \\ 0 & 0 & 1 \end{pmatrix}, \quad P_{\text{IH}} \equiv \begin{pmatrix} 1 & 0 & 0 \\ 0 & e^{-i\phi_1} & 0 \end{pmatrix}. \quad (4.3)$$

Here NH and IH stand for the normal and inverted hierarchy, respectively.

To proceed we choose a representative value  $M_H = 2$  GeV, and carry out a scan in the five-dimensional parameter space spanned by  $\Delta M \equiv M_3 - M_2$ ,  $\text{Re } z$ ,  $\text{Im } z$ ,  $\delta$ , and  $\phi_1$ .<sup>1</sup> A

---

<sup>1</sup>For  $\text{Re } z$  we restrict to a region continuously connected to  $\pi/2$  (another lies at around  $\text{Re } z = -\pi/2$ ).

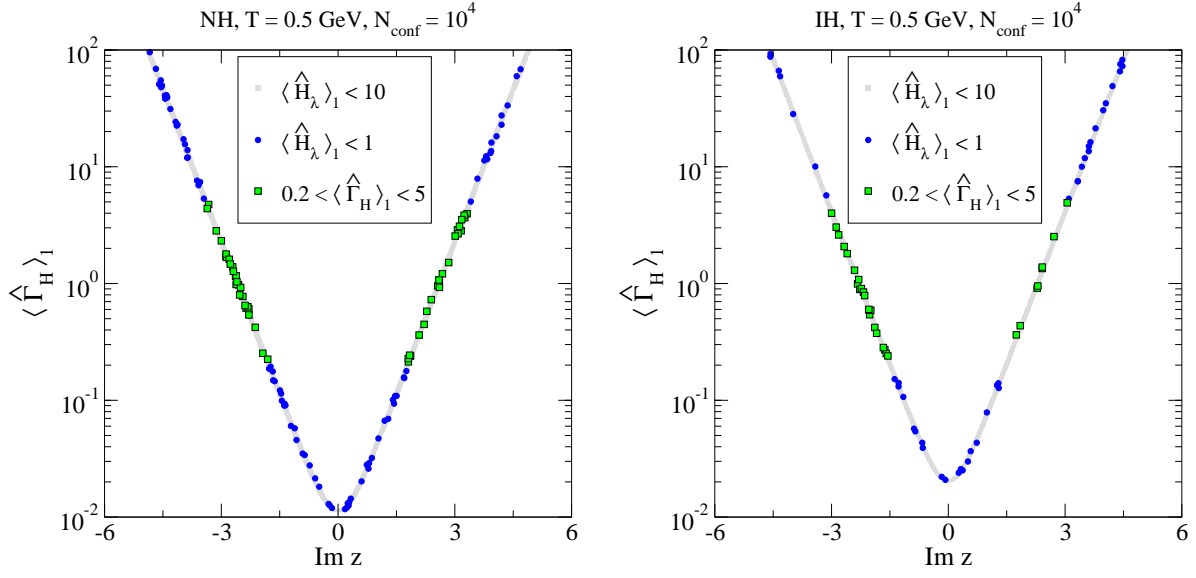


Figure 1: The distribution of  $\langle \widehat{\Gamma}_H \rangle_1$  as a function of  $\text{Im } z$ , with increasingly stringent constraints as indicated by the legend (left: normal hierarchy, right: inverted hierarchy).  $\langle \widehat{\Gamma}_H \rangle_1$  is strongly correlated with  $\text{Im } z$ , with the influence of the other parameters corresponding to the line width. For a rate not too slow or fast, we restrict to  $0.2 < \langle \widehat{\Gamma}_H \rangle_1 < 5.0$  (the points indicated with the green squares). As visible by the density of points, valid parameters are somewhat rarer for the inverted hierarchy.

random sample of data points is generated, with a logarithmic distribution in  $\Delta M$  and a flat one in the other parameters (restricting to  $|\text{Im } z| \leq 6.0$ ). The distributions in figs. 1–3 are based on  $\sim 10^4$  “accepted” points that satisfy the weak criterion  $\langle \widehat{H}_\lambda \rangle_1 < 10$  in terms of the low-energy constant defined in eq. (3.1). The criteria for a successful dark matter scenario are stronger than this, and reduce the data set to  $\sim 10^2$  points. We should clarify that these particular values are chosen for ease of illustration; many more points can be generated with minor cost but do not change the conclusions.

First, let us constrain  $\text{Im } z$  by considering  $\langle \widehat{\Gamma}_H \rangle_1$  from eq. (3.2). As shown in fig. 1, there is a near-perfect correlation of  $\langle \widehat{\Gamma}_H \rangle_1$  and  $\text{Im } z$ . We restrict to  $0.2 < \langle \widehat{\Gamma}_H \rangle_1 < 5.0$ , which delineates the range allowed for  $|\text{Im } z|$  accordingly.

Second, we constrain  $\langle \widehat{H}_\lambda \rangle_1$  from eq. (3.1) to lie within the range  $\langle \widehat{H}_\lambda \rangle_1 < 1$ . A full solution such as the one in sec. 5 shows that this is necessary for obtaining sufficient resonant enhancement of lepton asymmetry generation. As shown in fig. 2, this cuts the range allowed for  $\Delta M$  and  $\text{Re } z$  to an extremely narrow domain, which becomes an ellipse once the permitted range of  $\langle \widehat{\Gamma}_H \rangle_1$  is also taken into consideration.

Finally, in fig. 3, we show the low-energy constant  $\langle \widehat{\Gamma}_{\text{osc}} \rangle_1$  from eq. (3.3) as a function of the CP-violating phase  $\delta$ . The plot looks identical for  $\phi_1$ . Practically no correlation is observed, implying that many values of  $\delta$  and  $\phi_1$  are available. We have checked that these can then

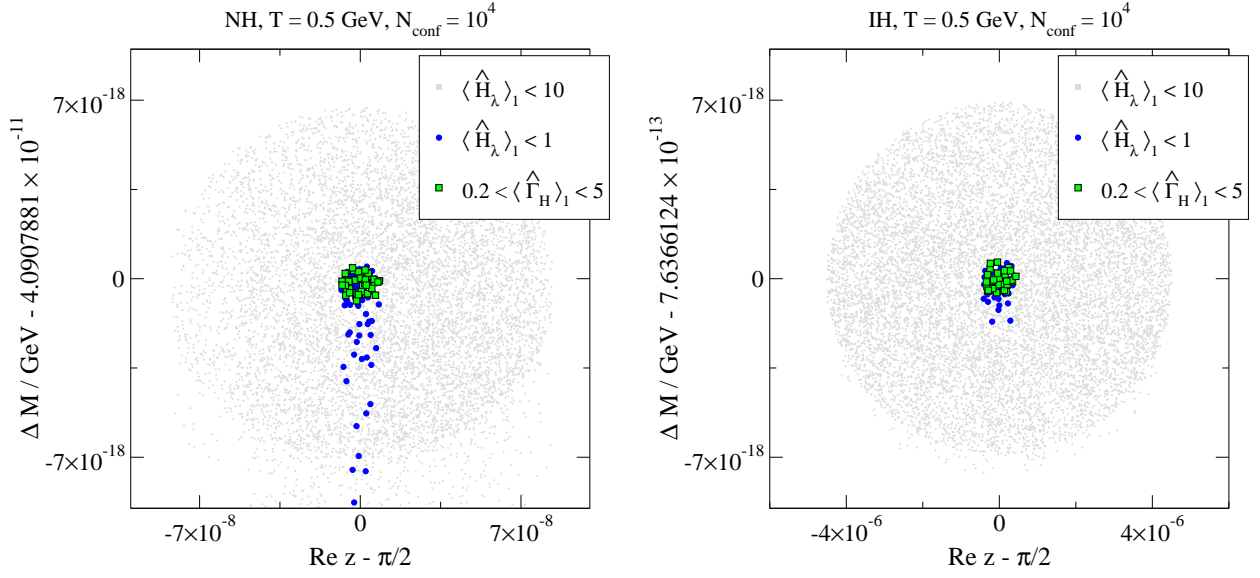


Figure 2: Points satisfying the increasingly stringent constraints indicated by the legend (cf. sec. 4.1), in the plane of  $\text{Re } z$  and  $\Delta M$  (left: normal hierarchy, right: inverted hierarchy). The narrow axis ranges illustrate the extraordinary degree of fine-tuning that is needed for realizing the desired scenario.

be tuned to produce the correct baryon asymmetry at  $T \sim 130$  GeV.

#### 4.2. Analytic estimates

The purpose of this section is to show that the features observed in figs. 1–3 can be understood analytically. To this end, let us start by noting that eqs. (3.1)–(3.3) involve summations over the active flavour  $a$  of a combination of Yukawa couplings and the rates  $\langle U_{(a)H}^+ \rangle_1$  and  $\langle Q_{(a)H}^\pm \rangle_1$ . At vanishing chemical potentials, only the masses of the charged leptons can lead to  $a$ -dependence. In the temperature range that we are interested in, this effect is in principle substantial for the  $\tau$ -lepton, however it originates through thermal corrections, which are suppressed. Therefore it is a good first approximation to treat the rates as flavour-independent. Then the active flavour sum over the neutrino Yukawas takes the form

$$\sum_a h_{Ia} h_{Ja}^* = \frac{1}{v^2} \left\{ \begin{array}{cc} M_2 [-\delta m \cos(2 \text{Re } z) + \bar{m} \cosh(2 \text{Im } z)] & \sqrt{M_2 M_3} [\delta m \sin(2 \text{Re } z) + i \bar{m} \sinh(2 \text{Im } z)] \\ \sqrt{M_2 M_3} [\delta m \sin(2 \text{Re } z) - i \bar{m} \sinh(2 \text{Im } z)] & M_3 [\delta m \cos(2 \text{Re } z) + \bar{m} \cosh(2 \text{Im } z)] \end{array} \right\}_{IJ}, \quad (4.4)$$

where

$$\bar{m} \equiv \sqrt{\Delta m_{31}^2} + \sqrt{\Delta m_{21}^2}, \quad \delta m \equiv \sqrt{\Delta m_{31}^2} - \sqrt{\Delta m_{21}^2} \quad (\text{NH}), \quad (4.5)$$

$$\bar{m} \equiv \sqrt{\Delta m_{23}^2} + \sqrt{\Delta m_{23}^2 - \Delta m_{21}^2}, \quad \delta m \equiv \sqrt{\Delta m_{23}^2} - \sqrt{\Delta m_{23}^2 - \Delta m_{21}^2} \quad (\text{IH}). \quad (4.6)$$



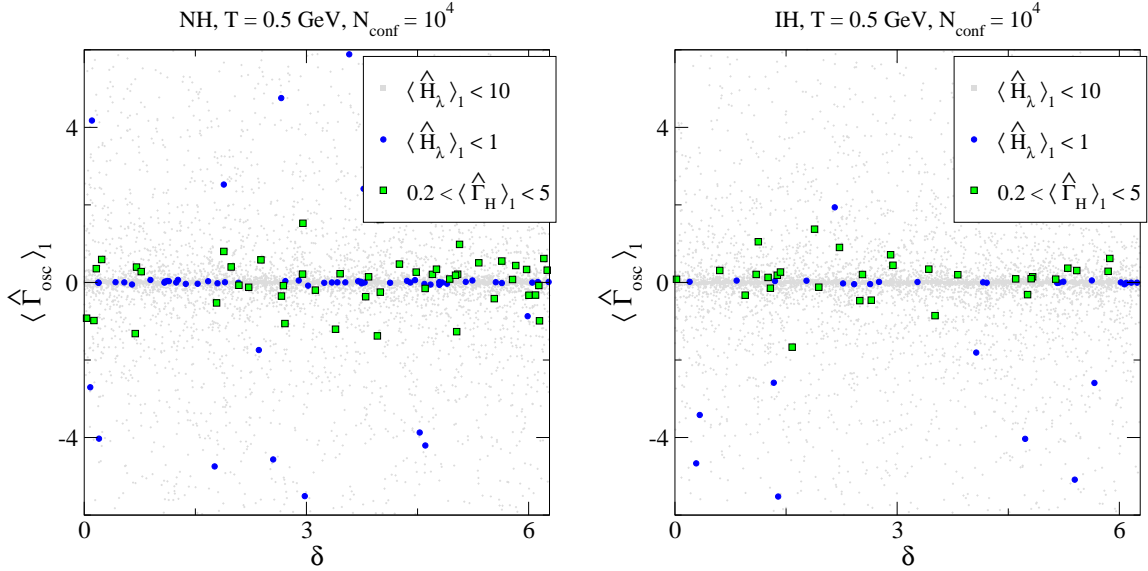


Figure 3: The distribution of  $\langle \hat{\Gamma}_{\text{osc}} \rangle_1$  as a function of  $\delta$  (left: normal hierarchy, right: inverted hierarchy). The effectively flat shape implies that dark matter production puts no constraint on  $\delta$ , and that therefore  $\delta$  can be tuned to obtain the correct baryon asymmetry. The same is true for  $\phi_1$ .

Here  $\Delta m_{ij}^2 \equiv m_i^2 - m_j^2$  are active neutrino mass differences, and we have employed the combinations appearing in standard fits ( $\Delta m_{21}^2 = \Delta m_{\text{sol}}^2$ ,  $\Delta m_{31}^2|_{\text{NH}} \approx \Delta m_{23}^2|_{\text{IH}} = \Delta m_{\text{atm}}^2$ ).

Let us now take eq. (3.1) and study its vacuum contributions, i.e. those of types (i) and (ii) in the language of sec. 3. This corresponds to taking

$$\langle U_{(a)H}^+ \rangle_1 \rightarrow -\frac{v^2}{2} \langle \omega_H^{-1} \rangle_1. \quad (4.7)$$

We can also write

$$\langle \omega_2 - \omega_3 \rangle_1 = \left\langle -\frac{2\Delta M M_H}{\omega_2 + \omega_3} \right\rangle_1 \approx -\Delta M M_H \langle \omega_H^{-1} \rangle_1. \quad (4.8)$$

Plugging eqs. (4.7) and (4.8) into eq. (3.1) and using eq. (4.4), the argument of the square root is a second order polynomial in  $\Delta M$ . It has a minimum for  $\Delta M = \Delta M_{\text{min}}$ , where

$$\Delta M_{\text{min}} = \frac{-2\delta m M_H \cos(2 \text{Re } z) [2M_H + \bar{m} \cosh(2 \text{Im } z)]}{[2M_H + \bar{m} \cosh(2 \text{Im } z)]^2 - \delta m^2 \sin^2(2 \text{Re } z)} \quad (4.9)$$

$$\approx -\delta m \cos(2 \text{Re } z) \left[ 1 - \frac{\bar{m} \cosh(2 \text{Im } z)}{2M_H} + \mathcal{O}\left(\frac{m_\nu^2}{M_H^2}\right) \right]. \quad (4.10)$$

In the final approximation we have kept the first correction in  $m_\nu/M_H$ , because it can be enhanced by the possibly large hyperbolic function.<sup>2</sup>

<sup>2</sup>We note that for very large Yukawas the Casas-Ibarra parametrization needs to be generalized [22].

Evaluating eq. (3.1) at the minimum given by eq. (4.10), we obtain

$$\langle \widehat{H}_\lambda \rangle_1 \Big|_{\Delta M = \Delta M_{\min}}^{(i)+(ii)} \approx \frac{\delta m M_H |\sin(2 \operatorname{Re} z)| \langle \omega_H^{-1} \rangle_1}{6c_s^2 H_T} \left[ 1 + \mathcal{O}\left(\frac{m_\nu^2}{M_H^2}\right) \right], \quad (4.11)$$

where we have again dropped higher-order terms in  $m_\nu/M_H$ . Noting that the values  $\operatorname{Re} z = 0 \bmod \pi$  are excluded by requiring  $\Delta M$  to be positive in eq. (4.10), we find that, as first shown in ref. [12], the cancellation between the (i) and (ii) contributions is largest — and the vacuum part of  $\langle \widehat{H}_\lambda \rangle_1$  is smallest — for  $\operatorname{Re} z = \pm\pi/2$ .

To see the extent of the cancellation, we may note that the (i) contribution evaluates for  $\Delta M = \Delta M_{\min}$  to

$$\langle \widehat{H}_\lambda \rangle_1 \Big|_{\Delta M = \Delta M_{\min}}^{(i)} \approx \frac{\delta m M_H |\cos(2 \operatorname{Re} z)| \langle \omega_H^{-1} \rangle_1}{6c_s^2 H_T} \left[ 1 + \mathcal{O}\left(\frac{m_\nu^2}{M_H^2}\right) \right]. \quad (4.12)$$

As  $\operatorname{Re} z$  approaches  $\pm\pi/2$ , the difference between eqs. (4.11) and (4.12) is maximized. It is for this reason that thermal corrections to  $\langle \widehat{H}_\lambda \rangle_1$ , of type (iii) in the language of sec. 3 and ordinarily suppressed by  $\sim (T/v)^4$ , are relatively speaking important when  $\Delta M \approx \Delta M_{\min}$ .

For fixed  $\operatorname{Re} z$ , the value of eq. (4.11) increases with decreasing temperature, because the Hubble rate shrinks and  $M_H \langle \omega_H^{-1} \rangle_1$  depends mildly on  $T$ . The thermal contribution (iii), on the other hand, increases with temperature. Hence,  $\langle \widehat{H}_\lambda \rangle_1$  exhibits a minimum as a function of temperature. The condition  $\langle \widehat{H}_\lambda \rangle_1 < 1$  at  $T = 0.5$  GeV ensures that this minimum is located where dark matter production is most efficient.

Fig. 2 can now be understood as follows. For  $|\operatorname{Im} z| \lesssim 3$ , the  $\cosh(2 \operatorname{Im} z)$  correction in eq. (4.10) is negligible, so that  $\Delta M_{\min} \approx -\delta m \cos(2 \operatorname{Re} z) \approx \delta m$ . This explains why most of the accepted points are symmetrically distributed around  $\operatorname{Re} z = \pi/2$ ,  $\Delta M = \delta m$ . The outliers below the center correspond to  $|\operatorname{Im} z| > 3$ , for which  $\langle \widehat{\Gamma}_H \rangle_1 \gtrsim 5$ . As shown by eq. (4.10), the correction from  $\cosh(2 \operatorname{Im} z)$  indeed reduces  $\Delta M_{\min}$ .

As far as the other parameters go, eq. (4.4) shows that  $\langle \widehat{\Gamma}_H \rangle_1$  and  $\langle \widehat{\Gamma}_{\text{osc}} \rangle_1$  are proportional to  $(\bar{m} M_H / v^2) \cosh(2 \operatorname{Im} z)$  and  $(\bar{m} M_H / v^2) \sinh(2 \operatorname{Im} z)$ , respectively. Indeed, fig. 1 is effectively a plot of the  $\cosh(2 \operatorname{Im} z)$  dependence, with the width of the line an indicator of the goodness of the flavour-independence approximation. The same approximation makes  $\langle \widehat{\Gamma}_{\text{osc}} \rangle_1$  independent of the phases  $\delta$  and  $\phi_1$ , as illustrated in fig. 3.

We end by noting that many more digits are shown on the vertical axes in fig. 2 than there are significant digits in  $\delta m$ , or that correspond to the theoretical uncertainties of the computation. Therefore the location of the optimal value of  $\Delta M$  is subject to uncertainty, however the degree of fine-tuning around this optimal value should be less so.

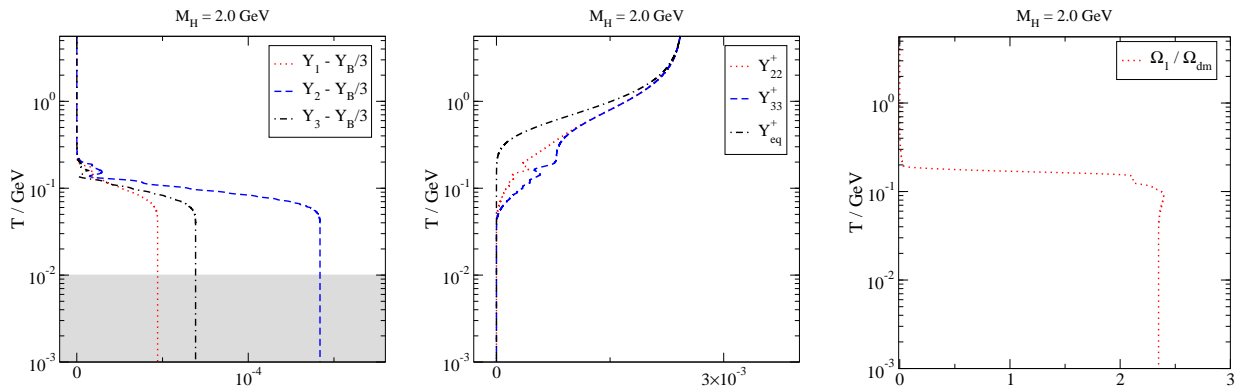


Figure 4: Example of a solution leading to a substantial dark matter abundance. Left: the evolution of lepton asymmetries. The grey band indicates the region in which active neutrino oscillations, not included in our solution, are expected to lead to flavour equilibration [24, 25]. Middle: diagonal components of the GeV-scale density matrix, compared with the equilibrium value  $Y_{eq}^+$  from eq. (2.1). Right: the fraction of dark matter that keV-scale sterile neutrinos account for, obtained from eq. (5.2). The minor decrease after obtaining the peak value is due to entropy dilution.

## 5. Example of a successful solution

We end by offering a “proof of existence” for a successful dark matter scenario. For this we consider the normal hierarchy of neutrino masses, and choose the parameters entering eq. (4.1) to lie within the domain found in fig. 2(left), *viz.*  $M_H = 2 \text{ GeV}$ ,  $\Delta M = 4.0907881 \times 10^{-11} \text{ GeV}$ ,  $z = 1.570796327 + 3.0i$ ,  $\delta = -1.88496$ ,  $\phi_1 = -0.07037$ . The low-energy constants of eqs. (3.1)–(3.3) evaluate at  $T = 0.5 \text{ GeV}$  to

$$\langle \hat{H}_\lambda \rangle_1 = 0.397, \quad \langle \hat{\Gamma}_H \rangle_1 = 2.323, \quad \langle \hat{\Gamma}_{osc} \rangle_1 = -0.800. \quad (5.1)$$

We have checked that these parameters leave behind the correct baryon asymmetry after its freeze-out at  $T \approx 130 \text{ GeV}$  [23],<sup>3</sup> and concentrate in the following on dark matter production. As dark matter production takes place at temperatures close to the QCD crossover and therefore contains substantial hadronic uncertainties, we choose to be conservative and even overproduce dark matter moderately.

As initial values for the lepton asymmetries we insert a “fixed-point” solution obtained in accordance with ref. [14],  $Y_a - Y_B/3 \approx 2.0 \times 10^{-8} \forall a$  at  $T \approx 5.6 \text{ GeV}$ . The dark matter mass is set to  $M_1 = 7 \text{ keV}$  and its Yukawa couplings to  $|h_{1a}| = 1.6 \times 10^{-13} \forall a$ .

The evolutions of the lepton asymmetries are shown in fig. 4(left), whereas the diagonal components of the GeV-scale density matrix can be found in fig. 4(middle). Lepton asym-

<sup>3</sup>In fact, the value is  $Y_B = 1.65 \times 10^{-10}$ , *i.e.* larger than the observed  $Y_B = 0.87 \times 10^{-10}$ , but the result is diluted by  $\sim 10\%$  due to the entropy release resulting from the freeze-out and decays of the GeV-scale sterile neutrinos. The remainder could be adjusted by tuning the CP-violating phases  $\delta$  and  $\phi_1$ .

metries of absolute magnitude  $\sim 10^{-4}$  can indeed be obtained, thanks to the fact that the density matrix falls out of equilibrium in a region where  $\langle \widehat{\Gamma}_{\text{osc}} \rangle_1$  is substantial.

When the temperature falls much below the mass of the GeV-scale sterile neutrinos, their density becomes Boltzmann-suppressed. Therefore the lepton number washout rate switches off, and lepton asymmetries become constant. At temperatures below  $T \sim 10$  MeV, lepton asymmetries would however evolve again, as active neutrino oscillations are expected to enforce flavour equilibrium [24, 25]. This effect has not been accounted for here, so the corresponding domain has been shaded in fig. 4(left). However, this does not affect dark matter production which has ceased at  $T \sim 100$  MeV.

The dark matter abundance is shown in fig. 4(right). From the helicity-averaged distribution  $f^+$  we compute the yield  $Y_{11}^+ \equiv \int_{\mathbf{k}} f^+ / s_T$  and subsequently estimate

$$\frac{\Omega_1}{\Omega_{\text{dm}}} \approx 4.57 \times Y_{11}^+ \times \frac{M_1}{\text{eV}}. \quad (5.2)$$

The data overshoot the correct value modestly, an effect which can easily be removed by a minuscule change of parameters such as  $\Delta M$  or  $\text{Re } z$  (cf. fig. 2).

## 6. Conclusions

By solving a set of coupled evolution equations for sterile neutrino density matrices and Standard Model lepton asymmetries at temperatures between 5.6 GeV and 1 MeV, we have scrutinized a proposal made in ref. [12] that this dynamics could lead to the generation of the correct dark matter abundance. As shown in fig. 4, we are happy to confirm the idea.

General features of solutions of the evolution equations can be understood in terms of a small number of low-energy constants, defined in sec. 3. As discussed in sec. 4.2 and illustrated numerically in fig. 2, it requires an exquisite degree of fine-tuning to set the low-energy constants in a domain leading to a solution like in fig. 4. This fine-tuning concerns particularly the Lagrangian mass difference  $\Delta M = M_3 - M_2$ , whose value needs to be small ( $< 0.1$  eV) and precisely chosen (to within  $\sim$  ppm), as well as the Casas-Ibarra angle  $\text{Re } z$ , which needs to be close to  $\pm \frac{\pi}{2}$ , and tuned to within a similar relative precision. We note that after a cancellation of  $\Delta M$  against Higgs vev and thermal corrections to the required degree, the physical mass splitting is  $< 10^{-7}$  eV.

In case these fine-tunings are not present, the dynamics in the chosen mass range generically leads to the generation of  $\sim 5 - 10\%$  of the observed dark matter abundance [18].

We should end with a word of warning, which is simultaneously a call for further work. The low-energy constant  $\langle \widehat{H}_\lambda \rangle_1$  defined in eq. (3.1) is small only if major cancellations between different contributions take place (cf. sec. 4.2). However, the individual contributions are only known within leading-order accuracy in Standard Model couplings. Higher-order corrections,

even if small for each contribution separately, are expected to be much larger than the remainder. Therefore, for *fixed* input parameters, the cancellation may be lifted by higher-order corrections. However, it should still be reachable if the input parameters are tuned slightly. It would be interesting to confirm this expectation by determining next-to-leading order corrections to thermal masses (which we have parametrized through the coefficient  $U_{(a)H}^+$ ), an exercise that has so far been carried out only for the helicity-conserving part of the interaction rates  $Q_{(a)H}^\pm$  at temperatures somewhat below the electroweak crossover [26].

## Acknowledgements

We are grateful to M. Shaposhnikov and I. Timiryasov for helpful comments on the manuscript. M.L. was partly supported by the Swiss National Science Foundation (SNF) under grant 200020B-188712.

## References

- [1] P. Minkowski,  $\mu \rightarrow e\gamma$  at a Rate of One Out of  $10^9$  Muon Decays?, Phys. Lett. B 67 (1977) 421.
- [2] M. Gell-Mann, P. Ramond and R. Slansky, *Complex Spinors and Unified Theories*, Conf. Proc. C 790927 (1979) 315 [1306.4669].
- [3] T. Yanagida, *Horizontal Symmetry and Masses of Neutrinos*, Prog. Theor. Phys. 64 (1980) 1103.
- [4] E. Bulbul *et al*, *Detection of An Unidentified Emission Line in the Stacked X-ray spectrum of Galaxy Clusters*, Astrophys. J. 789 (2014) 13 [1402.2301].
- [5] A. Boyarsky *et al*, *Unidentified Line in X-Ray Spectra of the Andromeda Galaxy and Perseus Galaxy Cluster*, Phys. Rev. Lett. 113 (2014) 251301 [1402.4119].
- [6] O. Ruchayskiy and A. Ivashko, *Restrictions on the lifetime of sterile neutrinos from primordial nucleosynthesis*, JCAP 10 (2012) 014 [1202.2841].
- [7] P. Hernández, M. Kekic and J. Lopez-Pavon,  *$N_{\text{eff}}$  in low-scale seesaw models versus the lightest neutrino mass*, Phys. Rev. D 90 (2014) 065033 [1406.2961].
- [8] E.K. Akhmedov, V.A. Rubakov and A.Y. Smirnov, *Baryogenesis via neutrino oscillations*, Phys. Rev. Lett. 81 (1998) 1359 [hep-ph/9803255].
- [9] T. Asaka and M. Shaposhnikov, *The  $\nu$ MSM, dark matter and baryon asymmetry of the universe*, Phys. Lett. B 620 (2005) 17 [hep-ph/0505013].
- [10] S. Alekhin *et al.*, *A facility to Search for Hidden Particles at the CERN SPS: the SHiP physics case*, Rept. Prog. Phys. 79 (2016) 124201 [1504.04855].
- [11] M. Shaposhnikov, *The  $\nu$ MSM, leptonic asymmetries, and properties of singlet fermions*, JHEP 08 (2008) 008 [0804.4542].

- [12] L. Canetti, M. Drewes, T. Frossard and M. Shaposhnikov, *Dark Matter, Baryogenesis and Neutrino Oscillations from Right Handed Neutrinos*, Phys. Rev. D 87 (2013) 093006 [1208.4607].
- [13] S. Eijima and M. Shaposhnikov, *Fermion number violating effects in low scale leptogenesis*, Phys. Lett. B 771 (2017) 288 [1703.06085].
- [14] J. Ghiglieri and M. Laine, *Precision study of GeV-scale resonant leptogenesis*, JHEP 02 (2019) 014 [1811.01971].
- [15] M. Laine and M. Shaposhnikov, *Sterile neutrino dark matter as a consequence of  $\nu$ MSM-induced lepton asymmetry*, JCAP 06 (2008) 031 [0804.4543].
- [16] J. Ghiglieri and M. Laine, *Improved determination of sterile neutrino dark matter spectrum*, JHEP 11 (2015) 171 [1506.06752].
- [17] D. Bödeker and A. Klaus, *Sterile neutrino dark matter: Impact of active-neutrino opacities*, 2005.03039.
- [18] J. Ghiglieri and M. Laine, *Sterile neutrino dark matter via GeV-scale leptogenesis?*, JHEP 07 (2019) 078 [1905.08814].
- [19] X.-D. Shi and G.M. Fuller, *A New dark matter candidate: Nonthermal sterile neutrinos*, Phys. Rev. Lett. 82 (1999) 2832 [astro-ph/9810076].
- [20] D. Bödeker and D. Schröder, *Kinetic equations for sterile neutrinos from thermal fluctuations*, JCAP 02 (2020) 033 [1911.05092].
- [21] J.A. Casas and A. Ibarra, *Oscillating neutrinos and  $\mu \rightarrow e\gamma$* , Nucl. Phys. B 618 (2001) 171 [hep-ph/0103065].
- [22] A. Donini, P. Hernández, J. López-Pavón, M. Maltoni and T. Schwetz, *The minimal 3+2 neutrino model versus oscillation anomalies*, JHEP 07 (2012) 161 [1205.5230].
- [23] M. D’Onofrio, K. Rummukainen and A. Tranberg, *Sphaleron Rate in the Minimal Standard Model*, Phys. Rev. Lett. 113 (2014) 141602 [1404.3565].
- [24] A.D. Dolgov *et al*, *Cosmological bounds on neutrino degeneracy improved by flavor oscillations*, Nucl. Phys. B 632 (2002) 363 [hep-ph/0201287].
- [25] Y.Y.Y. Wong, *Analytical treatment of neutrino asymmetry equilibration from flavor oscillations in the early universe*, Phys. Rev. D 66 (2002) 025015 [hep-ph/0203180].
- [26] G. Jackson and M. Laine, *A thermal neutrino interaction rate at NLO*, Nucl. Phys. B 950 (2020) 114870 [1910.12880].